

NO-A166 191

THE MELLIN TRANSFORM FILTER: A COMPUTER GENERATED
HOLOGRAM(U) ROYAL SIGNALS AND RADAR ESTABLISHMENT
MALVERN (ENGLAND) C L WEST AUG 85 RSRE-MEMO-3874

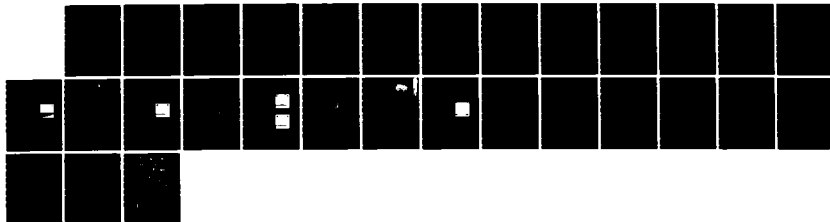
1/1

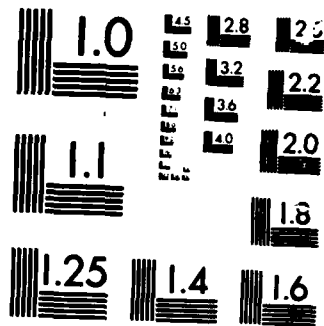
UNCLASSIFIED

DRIC-BR-98698

F/G 12/1

NL





MICROCOPY RESOLUTION TEST CHART

UNLIMITED

AD-A166 191

RSRE

MEMORANDUM No. 3374

ROYAL SIGNALS & RADAR ESTABLISHMENT

THE MELAN TRANSFORMER FILTERING UNIT
SEMICONDUCTOR HOLDING

Author: G. H. H.

PROCUREMENT EXECUTIVE
MINISTRY OF DEFENCE
JOSE W. W. W.
ADPCC

UNLIMITED

RSRE 16.01.1966. 191

UNLIMITED

ROYAL SIGNALS AND RADAR ESTABLISHMENT

Memorandum 3874

TITLE: THE MELLIN TRANSFORM FILTER: A COMPUTER GENERATED HOLOGRAM

AUTHOR: C L West

DATE: August 1985

SUMMARY

The procedure for designing a detour phase computer generated holograms is described with particular reference to a scale and rotation invariant transformation filter known as a Mellin transform filter. Experimental results are presented which demonstrate the main features of the devices.

Accession For	
NTIS GRA&I	<input checked="" type="checkbox"/>
DTIC TAB	<input type="checkbox"/>
Unannounced	<input type="checkbox"/>
Justification	
By	
Distribution/	
Availability Codes	
Dist	Avail and/or Special
A-1	



RSRE MEMORANDUM NO 3874

THE MELLIN TRANSFORM FILTER: A COMPUTER GENERATED HOLOGRAM

C L West

LIST OF CONTENTS

- 1 Introduction
- 2 Continuous Phase Description for a Mellin Transform Filter: Theory
- 3 The Binary Fraunhofer Hologram and the Mellin Transform Filter
- 4 Experimental Results
- 5 Conclusion

Acknowledgements
References

LIST OF FIGURES

- 1 Definition of cell apertures in detour phase computer generated holograms
- 2 Mellin transform filters used in the experiments
- 3 Experimental arrangement for employing Mellin transform filters
- 4 Mellin No 1: fully illuminated
- 5 Mellin No 1: circular aperture on and off axis
- 6 Mellin No 1: circular annulus
- 7 Mellin No 1: half circular annulus at various orientations
- 8 Mellin No 1: square annulus at various orientation
- 9 Mellin No 1: square annulus - off axis - 0 rotation
- 10 Mellin No 1: square annulus - off axis $\pi/4$ rotation
- 11 Mellin No 3: fully illuminated

LIST OF APPENDICES

- A Some alternative geometric transformations using computer generated hologram
- B Parameters and programs used to define the Mellin transform filters described in the text

1 INTRODUCTION

Coherent optical systems possess the great qualities of high data throughput with parallel processing. In the last few years several areas which utilise these qualities have developed and are becoming increasingly important with the development of high resolution holographic film and real time coherent light valves. Phase masks which were not possible to achieve using purely optical systems are now being developed using the various techniques of computer generated holography⁽¹⁻¹⁰⁾. Likewise real time optical correlator systems have been demonstrated using the new generation of optical light valves. The two main optical correlators that are usually demonstrated are the frequency plane correlator and the joint transform correlator. Both of these systems exhibit spatial invariance but are sensitive to scale and rotation. In 1983 Saito et al⁽¹⁾ described a scale and rotation invariant real time optical correlator which employed a Mellin transform phase mask. The purpose of this memorandum is to describe the methods employed to create this Mellin transform filter and to discuss some of its limitations. During this exercise it is hoped that the reader will obtain some insight into the field of computer generated holograms.

2 CONTINUOUS PHASE DESCRIPTION FOR A MELLIN TRANSFORM FILTER: THEORY

Consider the Fourier transform properties of a simple lens. The light intensity in the front focal plane of a lens, $F(u,v)$, is related to the light intensity in the rear focal plane, $f(x,y)$, by the relationship

$$F(u,v) = \iint f(x,y) \exp(-jkxu/f) \exp(-jkyv/f) dx dy \quad (1)$$

where f is the focal length of the lens and $k = 2\pi/\lambda$, λ is the wavelength of the light. In our particular case we consider an initial input function which has only amplitude information, the phase content of the function $f(x,y)$ is supplied by a phase plate that is coplanar with this input function, thus $f(x,y) = g(x,y) \exp(j\phi(x,y))$ and

$$F(u,v) = \iint g(x,y) \exp(j(\phi(x,y) - kxu/f - kyv/f)) dx dy \quad (2)$$

By applying the method of stationary phase to evaluate this integral it can be shown that the point (x,y) of plane $f(x,y)$ is mapped into the point (u,v) of plane $F(u,v)$ by the following relationships

$$u = \frac{\lambda f}{2\pi} \frac{\partial \phi}{\partial x}(x,y) \quad v = \frac{\lambda f}{2\pi} \frac{\partial \phi}{\partial y}(x,y) \quad (3)$$

For a continuous phase computer generated hologram we require that the functions u and v have continuous partial derivatives in a simply connected region of plane $f(x,y)$. This implies

$$\frac{\partial u}{\partial y} = \frac{\partial v}{\partial x} \quad \text{or} \quad \frac{\partial}{\partial y} \left(\frac{\partial \phi}{\partial x} \right) = \frac{\partial}{\partial x} \left(\frac{\partial \phi}{\partial y} \right) \quad (4)$$

In most cases of computer generated holograms the mapping that is required is defined and it is necessary to calculate the appropriate phase function

$\phi(x,y)$ using equation (3) (subject to the continuous phase conditions of equation (4)). In Appendix A the case is considered when equation (4) is not satisfied.

In the present case we choose the mapping

$$\begin{pmatrix} x \\ y \end{pmatrix} \rightarrow \begin{pmatrix} u \\ v \end{pmatrix} = \begin{pmatrix} \ln(r) \cdot s \\ -\theta s \end{pmatrix} = \begin{pmatrix} \ln(x^2+y^2) \cdot s/2 \\ -\tan^{-1}(y/x) \cdot s \end{pmatrix} \quad (5)$$

Careful evaluation of equation (4) confirm that this function does indeed produce a continuous phase function and solving the two differential equations (3) yield the final form of the phase function (Ref 1)

$$\phi(x,y) = -\frac{2\pi s}{\lambda f} \left\{ y \tan^{-1}\left(\frac{y}{x}\right) - \frac{x}{2} \ln(x^2+y^2) + x + \pi y H(-x) \right\} \quad (6)$$

where s is a scaling factor and $H(-x)$ is the unit step function which has the following definition

$$\begin{aligned} H(-x) &= 1 & x < 0 \\ H(-x) &= 0 & x > 0 \end{aligned} \quad (7)$$

3 THE BINARY FRAUNHOFER HOLOGRAM AND THE MELLIN TRANSFORM FILTER

A binary hologram consists of transparent dots on an opaque background: the transmittance of the medium being either one or zero at all places on the transparency^(4,5). In order that a complex amplitude $f(x,y)$ can be realised on the hologram we must consider how phase information can be recorded. There are three ways in which the phase of a light wave can be influenced: retardation while travelling through a dielectric, phase jump at reflection and detour phase. The mechanism of detour phase can be visualised using the description of grating diffraction. In the first order diffraction pattern light from adjacent slits have a relative 2π phase shift, this is the detour phase and if the relative centres of the slits are not correctly placed it is clear that an alternative value for the detour phase can be realised.

In the synthesis of the complex filter function it is assumed that the cells are of such a size, $(\Delta x)^2$, that the function $f(x,y)$ will almost be constant across the cell

$$f(x,y) \simeq f(n\Delta x, m\Delta y) = f_{nm} = A_{nm} \exp(j\phi_{nm}) \quad (8)$$

The cells may also be so small that the envelope function that they add to the waveform is unimportant. Several ways of implementing the phase and amplitude information have been tried. For the Mellin transform filters in this memorandum the schemes shown in Figure 1 have been used. The simplest case consists of a slit whose width is half of the cell size and whose height is normalised so that the maximum amplitude required by the function corresponds exactly to the cell height. The position of this element relative to the centre of the cell is a measure of the detour phase required of this element. One disadvantage of this scheme is that there is a slight possibility of the contribution from adjacent cells overlapping. This may be overcome by folding the aperture round within the cells so that we effectively either add or subtract 2π from the detour phase of the contribution outside the cell to bring it back within the cell walls (see Figure 1).

When diffracted light from a regular array of cells of dimension Δx is collected by a lens of focal length f , the diffraction pattern seen in the focal plane of this lens is a regular square array of points where the separation of the points Δu is given by

$$\Delta u = \frac{\lambda}{\Delta x} f = \Delta v \quad (9)$$

We have chosen to map the (x,y) plane to the (u,v) plane in such a way that a rotation of an object about the origin by an angle θ in the (x,y) plane will correspond to a linear shift of θs in the v direction of the (u,v) plane. We choose, therefore, the size of the cells in the hologram to be such that the separation of the diffraction orders Δv in the (u,v) plane to correspond to an integer multiple of $2\pi s$, the linear shift introduced in the v direction due to complete rotation of the image in the (x,y) plane.

In this way the diffraction order spots will give a direct calibration of θ and $\ln(r)$ in the (u,v) field. Thus

$$\Delta y = \Delta x = \frac{\lambda f}{2\pi ns} = \frac{\lambda f}{\Delta u} = \frac{\lambda f}{\Delta v} \quad (10)$$

all linear dimensions are measured in the same units. Next we choose the separation of the orders in the (u,v) plane to be 5 mm, a convenient size to image on our TV system. Thus $\Delta v = 5 = 2\pi s$. The parameter s therefore takes the values $(5/2\pi)$ and $(1/2\pi)$ respectively for the two conditions ($n=1$) and ($n=5$) considered in the experiments (using equation (10)). For $\lambda = 514.5 \times 10^{-6}$ mm and $f = 1000$ mm the above choice of Δv corresponds to a cell size in the hologram of 102.9 μ m square.

The Mellin transform filter that would be produced using these parameters was simulated using the 'basic' program included in Appendix B. It is clear from these programs that an amplitude term has been included in the plot. The Mellin filter is a phase-only mask and the amplitude term is included so that a linear magnification of the input image will result in a corresponding shift in the output pattern but will have no resulting change of intensity of the transform image. In the absence of such a term a magnified input image would have a transformed image that was much brighter. This is not desirable when the detecting system may have a limited dynamic range and where one would wish to define a suitable operating point that is invariant with respect to scale. As an image intensity will scale according to an r^2 term with respect to iniform illumination, the amplitude term must vary as r^{-1} (the amplitude in our plots is set arbitrarily to unity for $r \leq 1$ mm, and scaled as $1/r$ for $r > 1$ mm). The resulting filters are shown in Figure 2. The final holograms were produced using the Electromask facility at RSRE. This facility has a minimum slit of 2.6 μ m and a maximum slit of 1.5 mm. The positioning accuracy of the slit is 0.25 μ m over a 60 mm field. The size of transform filter we can reasonably produce is limited by the writing speed of the electromask (4 k/hr for chrome masks, 16 k/hr for emulsion masks). For our particular device the write time of between 2 and 8 hours was required for the 3×10^4 images.

4 EXPERIMENTAL RESULTS

The first Mellin transform filter (MELLIN No 1) has been used to demonstrate the $\ln(r)$ - θ transformation in various situations. All of the experimental results were taken using the system depicted in Figure 3. Light from an Argon ion laser is spatially filtered and collimated on to the transform filter which is in the near focal plane of a 1 m focal length achromatic doublet lens. The lens collects the light and focusses it on to the active surface of a lowlight TV camera which lies in the front focal plane of the lens. The image is then displayed on a suitable monitor. Amplitude modulated input data is placed just behind the Mellin filter in the collimated light.

The active area of the filter has a 10.29 mm radius. Illumination of the whole of this area corresponds to a band in the $\ln(r)$ - θ plane as depicted in Figure 4. This defines the region of the transform plane (u,v) that meaningful results can be measured. The upper edge of the illuminated region of the (u,v) plane corresponds to $r = 10.29$ ($\ln(r) = 2.33 = 0.74\pi$). Correspondence between the theory and experiment can be seen to be very good.

When the aperture has a restricted outer radius the upper edge of the image in the transform plane lowers (see lower part of Figure 5). If the lower radius of the image is also restricted so that the filter is illuminated by a circular annulus (Figure 6) then the transformed image becomes a narrow band in the (u,v) plane whose width is given by $\ln(b/a)$ where a and b are the inner and outer radii respectively. If this circular annulus is further restricted so that only a half of the aperture is transparent (Figure 7) the image becomes restricted in the θ -direction also. Figure 7 demonstrates the effect of rotation of the circular half annulus on the transformed image. It is apparent that the major effect is not in the fine detail of the image but is merely a translation of the same image along the θ axis. This overcomes one of the problems of the space invariant transform - namely that of invariance to rotation. This effect is further demonstrated in Figure 8 with a full square annulus. In this case the peak features, corresponding to the corners of the square, shift by $\pi/4$ in the transform plane upon a rotation of the illuminating image by a similar amount. Note also in this figure the multiple diffraction pattern associated with the cell diffraction spots. This pattern is a replicated version of the pattern that one would observe at the centre of the transform plane if a single cell of dimensions Δx^2 is placed in the input plane, and is useful in confirming the orientation of the square annulus with respect to the Mellin axes.

When an image is no longer on axis and does not even include the origin in the x,y plane, the pattern in the transform plane is very different. For a circular aperture (Figure 5) the pattern is an oblated circle whose size and distortion depends on its position with respect to the (x,y) origin. If a more complex shape, eg the square annulus, is taken off axis its pattern depends strongly on the orientation of the square with respect to the Mellin axes. Two such cases are shown in Figure 9 and Figure 10 for two orientations of the square which differ by a rotation of $\pi/4$. The patterns are obviously very different although the same shape is employed but the correspondence between experiment and theory is still excellent. This demonstrates the fact that the Mellin transform can only show rotation invariance with respect to its own centre - not the centre of the concerned object that illuminates the filter. This is a particularly important point with respect to use of the filter in a correlator system - obviously targets of interest must be aligned before analysis if this scheme is to be used.

In this section experimental data has only been displayed for the first Mellin transform filter (Mellin No 1). An improved version of this filter was constructed (Mellin No 3) using the alternative method of CGH construction shown in Figure 1. The filter itself looks more aesthetically pleasing to the eye (see Figure 2) showing no large gaps in the filter and displaying a more continuous form. Experimentally however there is only marginal improvement in performance using this filter and so no data is presented. This lack of significant improvement is probably due to the sampling conditions of the object (ratio of the cell size to object size) remaining the same for the two filters. An alternative filter (Mellin No 2) hoped to overcome some of the problems incurred due to the near undersampling of the phase function by the previous two holograms. The phase function was expanded by a factor of 5 and this resulted in a contraction of the output image of a similar factor (Figure 11). In Figure 11 we note that the θ field does not appear to be symmetrical about the diffraction orders. At first this may appear to be incorrect but if the form of the phase function is reconsidered (equation (6)) it is noted that images in the 2nd and 3rd input quadrants (negative x) have an additional linear phase term. This linear term acts like a single sideband modulator shifting the field produced by these two quadrants to an asymmetric position about the final diffraction pattern. The magnitude of this shift is such that the field for positive x and negative x meet precisely. In practice this effect is of little consequence as it only produces a linear shift of the output plane.

5 CONCLUSIONS

The use of a detour phase computer generated hologram to provide a phase plate which can produce a given transformation has been demonstrated. The filter, when used in conjunction with the appropriate coherent light and lens of correct focal length, has been shown to produce an output image whose shape is independent of magnification and rotation about the transform filter origin. This filter may be of significant use in particular areas of optical signal processing where the direction of the image is known in advance (otherwise a raster type scan must be employed). Of the three filters most of the experimental data displayed in this memorandum was obtained using Mellin No 1. An improved version of the filter using a modified plotting routine (Mellin No 3, Figures 1 and 2) showed no significant advantage over the first type. It is true that the improved filter is aesthetically better with regard to the absence of obvious errors in the phase description but the limited number of cells that describe particular images still results in some distortion of the images, especially with regard to the 0 and π positions in the transform plane. Similarly the modified plotting routine that described the filter with a slower varying phase characteristic shared no significant improvement. This once more was probably due to a similar number of cells still being used to describe the same images. The major experimental difference between Mellin No 2 and Mellin Nos 1, 3 was the reduction in the output plane that was usefully employed (Figure 11).

We have chosen to implement these filters using binary computer generated holographic techniques. As only phase only functions are used in these filters it may be more appropriate to develop future filters using alternative techniques, eg Referenceless On-Axis Complex Hologram (ROACH)⁽⁷⁾. These techniques have the advantages of high efficiency and that of the transformation being directed on-axis and not to the first order diffraction pattern.

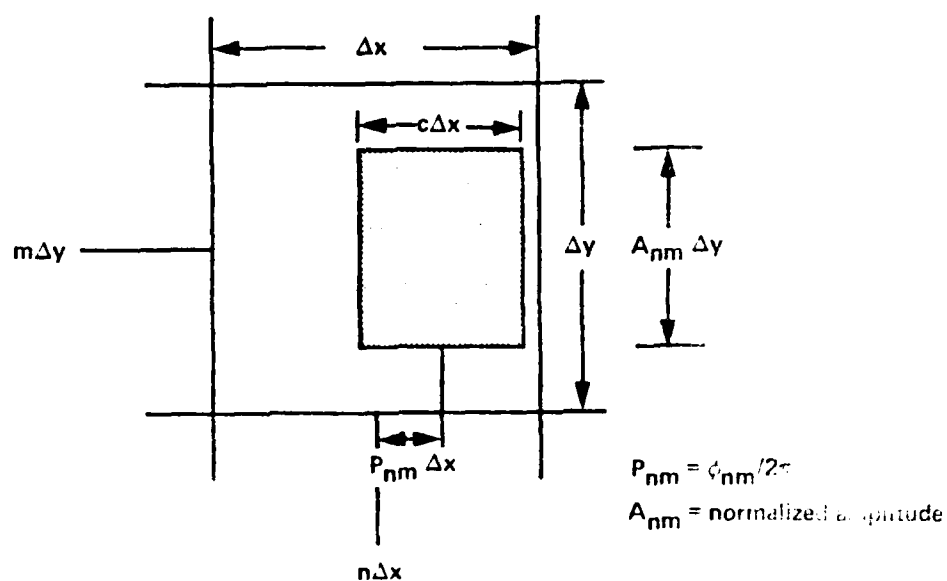
ACKNOWLEDGEMENTS

I would like to thank M Hepplewhite and G K Gibbons who assisted in the production of these filters and the following people for useful discussions: M F Lewis, M S Hazell (RSRE); T J Hall, M A Fiddy and W J Hossack (Kings College).

REFERENCES

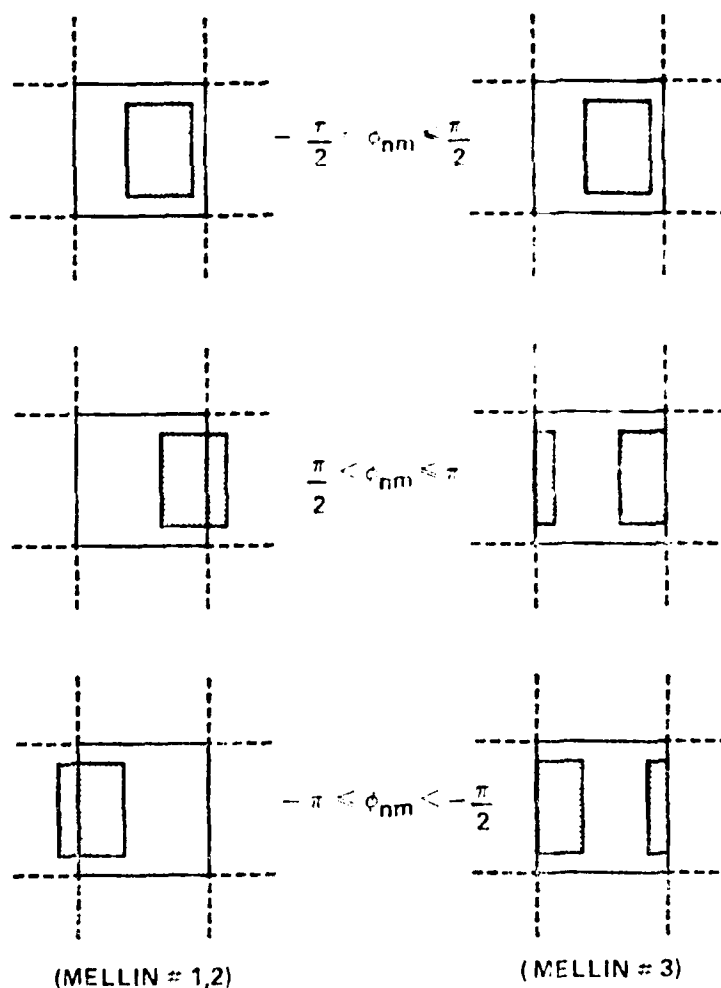
- 1 Saito Y, Komatsu S and Ohzu H; "Scale and rotation invariant real time optical correlator using computer generated hologram", Optics Communication Vol 47, No 1, 1983, pp 8-11.
- 2 Cederquist J and Tai A M; "Computer generated holograms for geometric transformations", Applied Optics, Vol 23, No 18, 1984, pp 3099-3104.
- 3 Bryngdahl O; "Optical map transformations", Optics Communication Vol 10, No 2, 1974, pp 164-168.
- 4 Brown B R and Lohmann A W; "Complex spatial filtering with binary masks" Applied Optics, Vol 5, No 6, 1966, pp 967-969.
- 5 Lohmann A W and Paris D P; "Binary Fraunhofer Holograms, generation by computer", Applied Optics, Vol 6, No 10, 1967, pp 1739-1748.
- 6 Hauck R and Bryngdahl O, "Computer generated holograms with pulse density modulation", J Opt Soc Am A, Vol 1, No 1, 1984, pp 5-10.
- 7 Mountain G D, Ward J F L and Burge R E, "Evaluation of a method for producing on-axis complex computer generated holograms", I: Optik 61, No 3, 1982, pp 263-272; II: Optik 61, No 4, 1982, pp 335-348.
- 8 Horner J L and Gianino P D, "Phase only matched filtering", Applied Optics, Vol 23, No 6, 1984, pp 812-816.
- 9 Lee W H, "Computer generated holograms: techniques and applications", Progress in Optics 16 (1978) pp 121-232.
- 10 Haugen P R, Bartelt H and Case S K; "Image formation by multifacet holograms", Applied Optics, Vol 22, No 18, Sept 1983, pp 2822-2829.

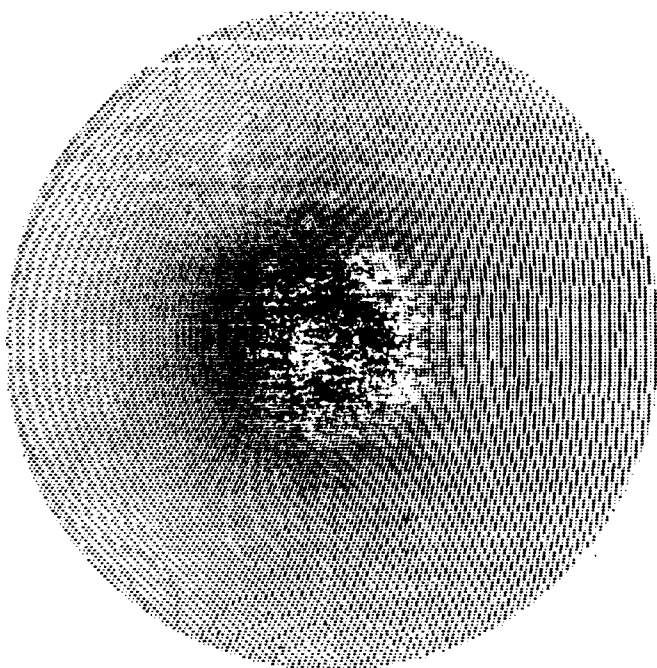
FIGURE 1 DEFINITION OF CELL APERTURES FOR REALIZING COMPLEX GENERATED HOLOGRAMS USING THE DETOUR PHASE METHOD



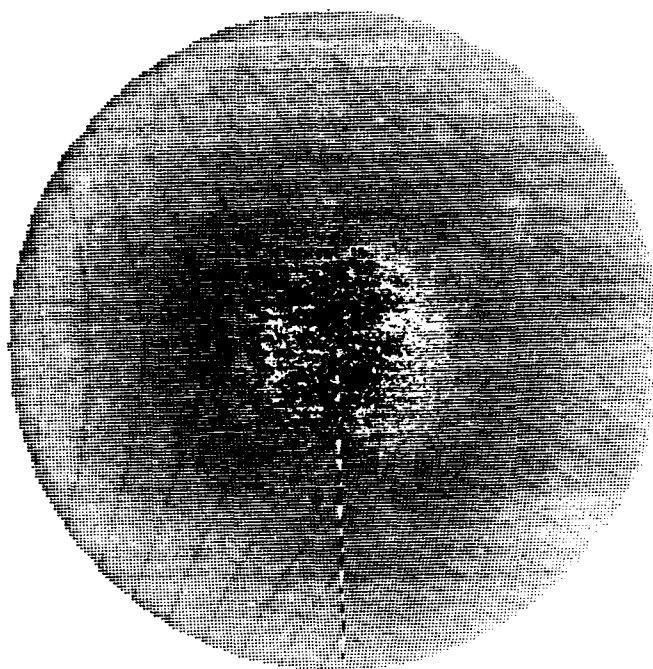
CASE I; $c = 0.5$

CASE II; $c = 0.5$

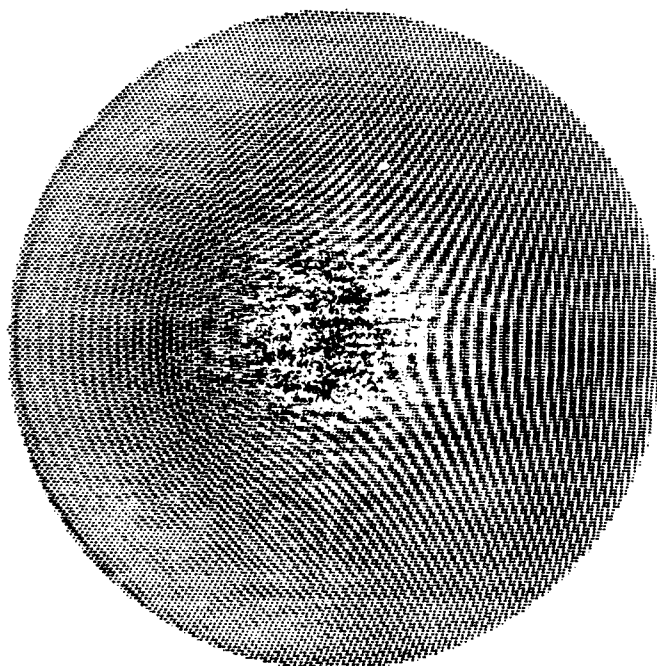




MELLIN # 1



MELLIN # 2



MELLIN # 3

FIGURE 2

MELLIN TRANSFORM FILTERS (NEGATIVE)

EXPERIMENTAL ARRANGEMENT USED TO CONFIRM
OPERATION OF MELLIN TRANSFORM FILTERS

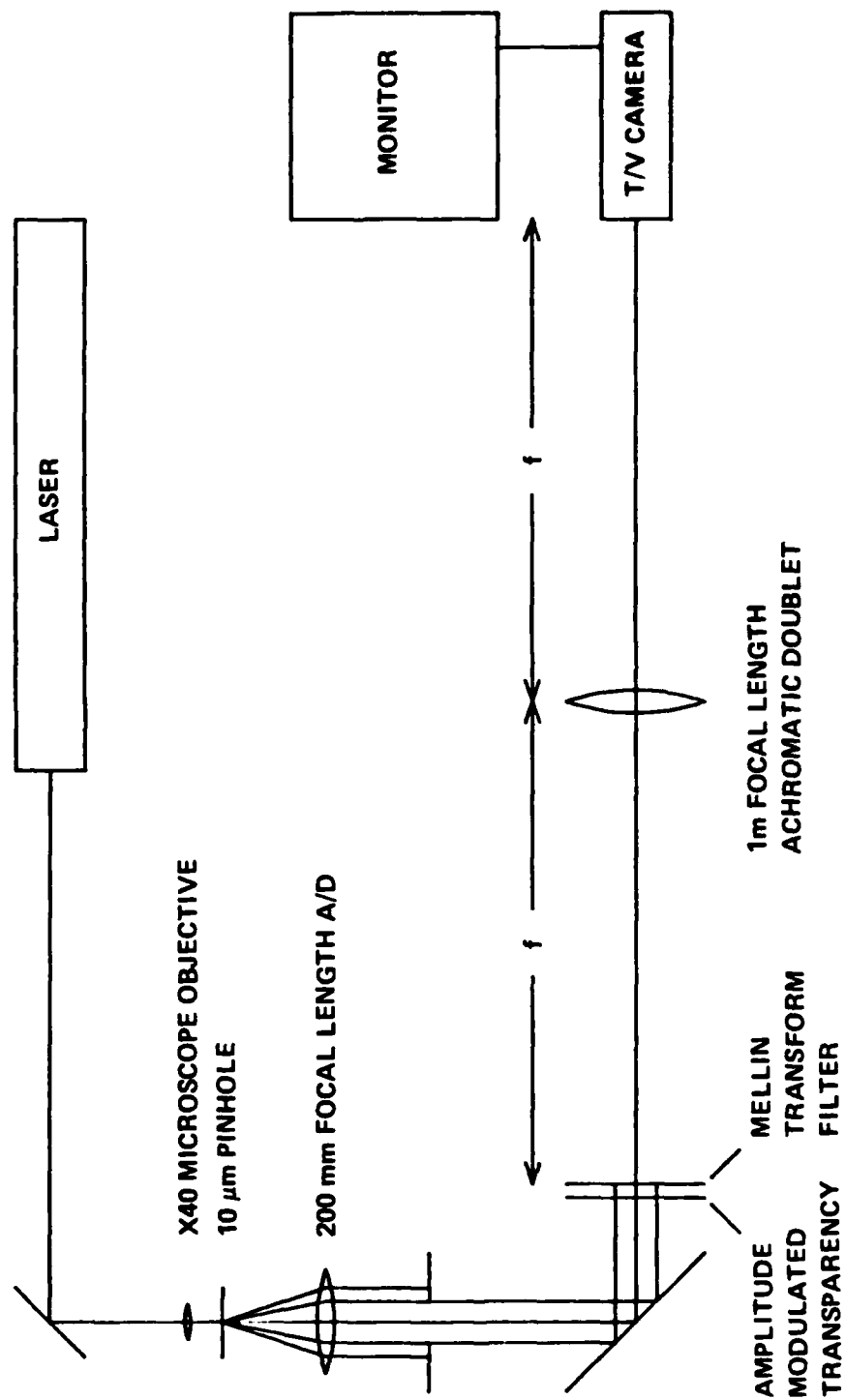


FIGURE 3

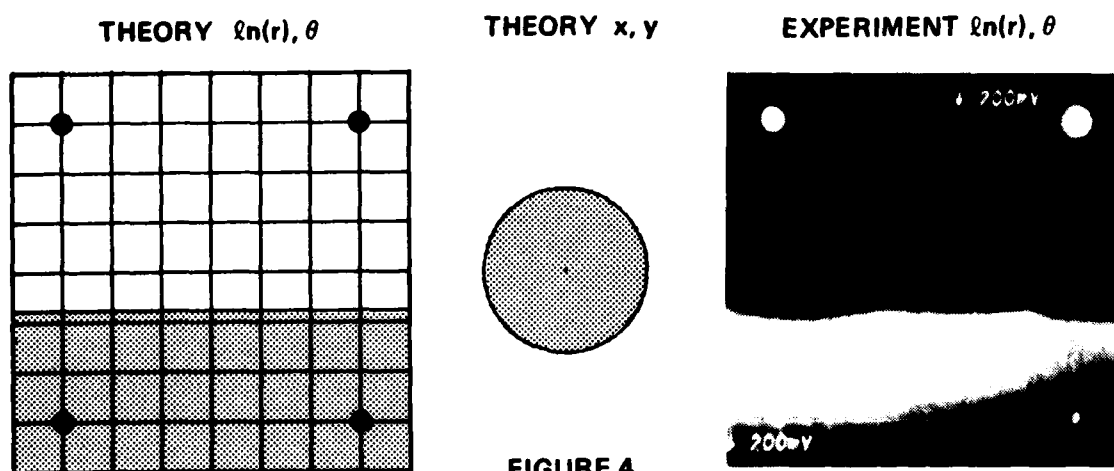
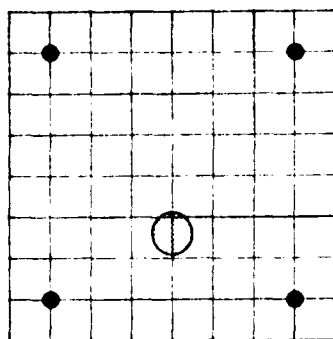
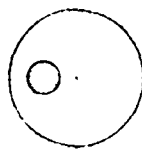


FIGURE 4

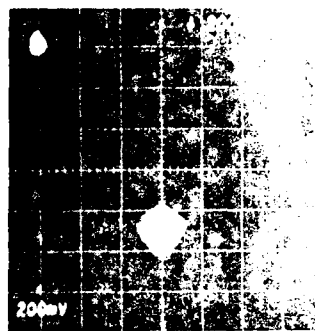
THE MELLIN TRANSFORM FILTER (MELLIN #1) FULLY ILLUMINATED. COMPARISON OF EXPERIMENTAL DATA WITH THEORY. EACH SQUARE HAS DIMENSIONS OF $\pi/3$ IN EACH DIRECTION. $\ell n(r)$ IS PLOTTED VERTICALLY, θ HORIZONTALLY. THE DOTS CORRESPOND TO THE DIFFRACTION PATTERN FROM THE CELL SIZE USED IN THE COMPUTER GENERATED HOLOGRAM



THEORY $\{n(r), \theta$



THEORY x, y



EXPERIMENT $\{n(r), \theta$

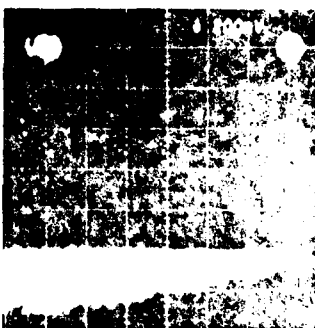
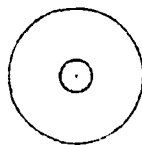
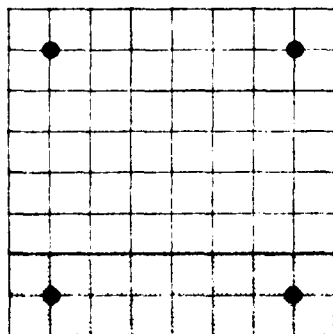
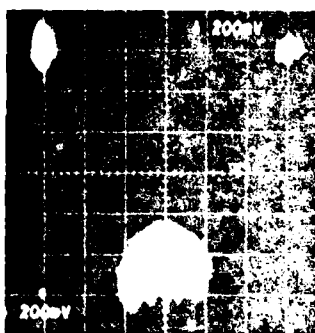
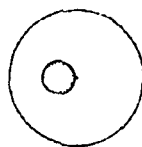
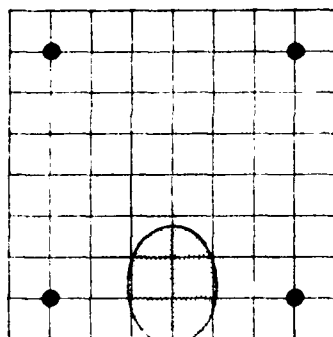
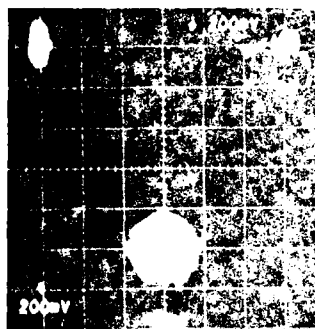
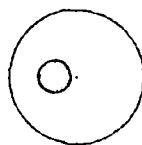
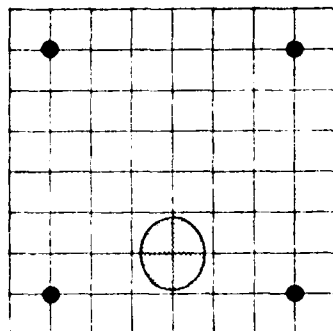
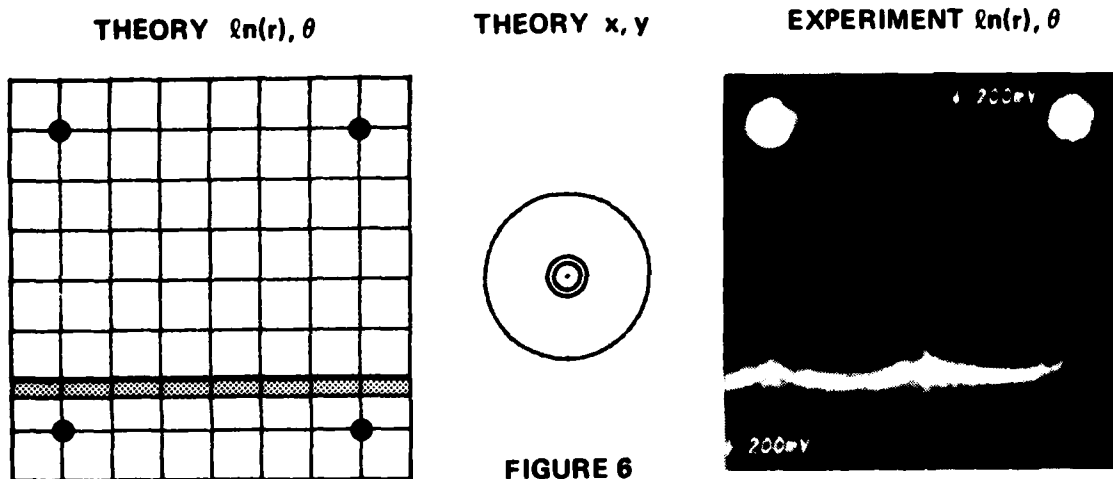
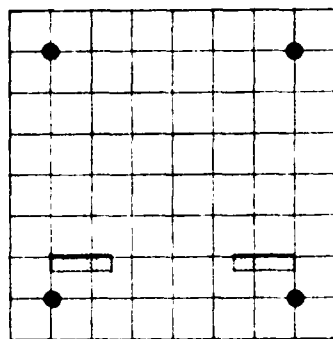


FIGURE 5

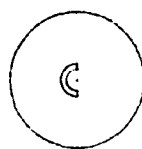
THE MELLIN TRANSFORM FILTER (MELLIN #1) ILLUMINATED BY A CIRCULAR APERTURE OFF AND ON AXIS. COMPARISON OF EXPERIMENTAL DATA WITH THEORY. EACH SQUARE HAS DIMENSIONS OF $\pi/3$ IN EACH DIRECTION. $\{n(r)\}$ IS PLOTTED VERTICALLY, θ HORIZONTALLY. THE DOTS CORRESPOND TO THE DIFFRACTION PATTERN FROM THE CELL SIZE USED IN THE COMPUTER GENERATED HOLOGRAM



THE MELLIN TRANSFORM FILTER (MELLIN #1) ILLUMINATED BY A CIRCULAR ANNULUS ON AXIS. COMPARISON OF EXPERIMENTAL DATA WITH THEORY. EACH SQUARE HAS DIMENSIONS OF $\pi/3$ IN EACH DIRECTION. $\ln(r)$ IS PLOTTED VERTICALLY, θ HORIZONTALLY. THE DOTS CORRESPOND TO THE DIFFRACTION PATTERN FROM THE CELL SIZE USED IN THE COMPUTER GENERATED HOLOGRAM



THEORY $n(r), \theta$



THEORY x, y



EXPERIMENT $n(r)$

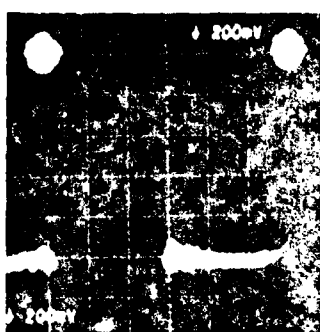
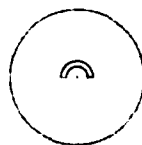
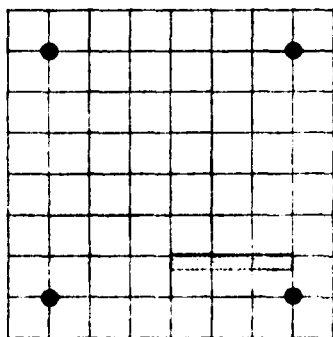
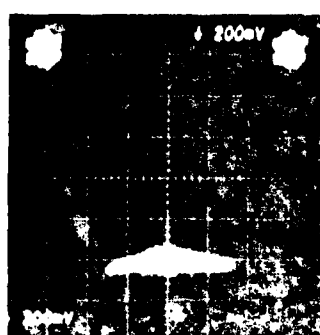
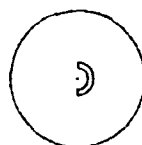
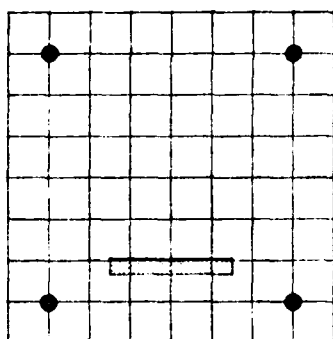
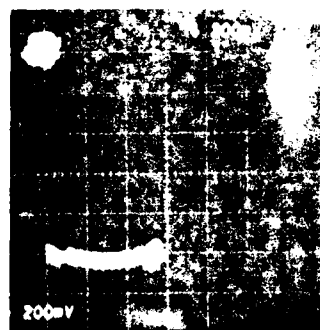
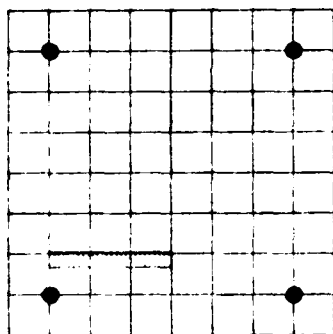


FIGURE 7

THE MELLIN TRANSFORM FILTER (MELLIN #1) ILLUMINATED BY A HALF CIRCULAR ANNULUS ON AXIS AT VARIOUS ORIENTATIONS. COMPARISON OF EXPERIMENTAL DATA WITH THEORY. EACH SQUARE HAS DIMENSIONS OF $\pi/3$ IN EACH DIRECTION. $n(r)$ IS PLOTTED VERTICALLY, θ HORIZONTALLY. THE DOTS CORRESPOND TO THE DIFFRACTION PATTERN FROM THE CELL SIZE USED IN THE COMPUTER GENERATED HOLOGRAM

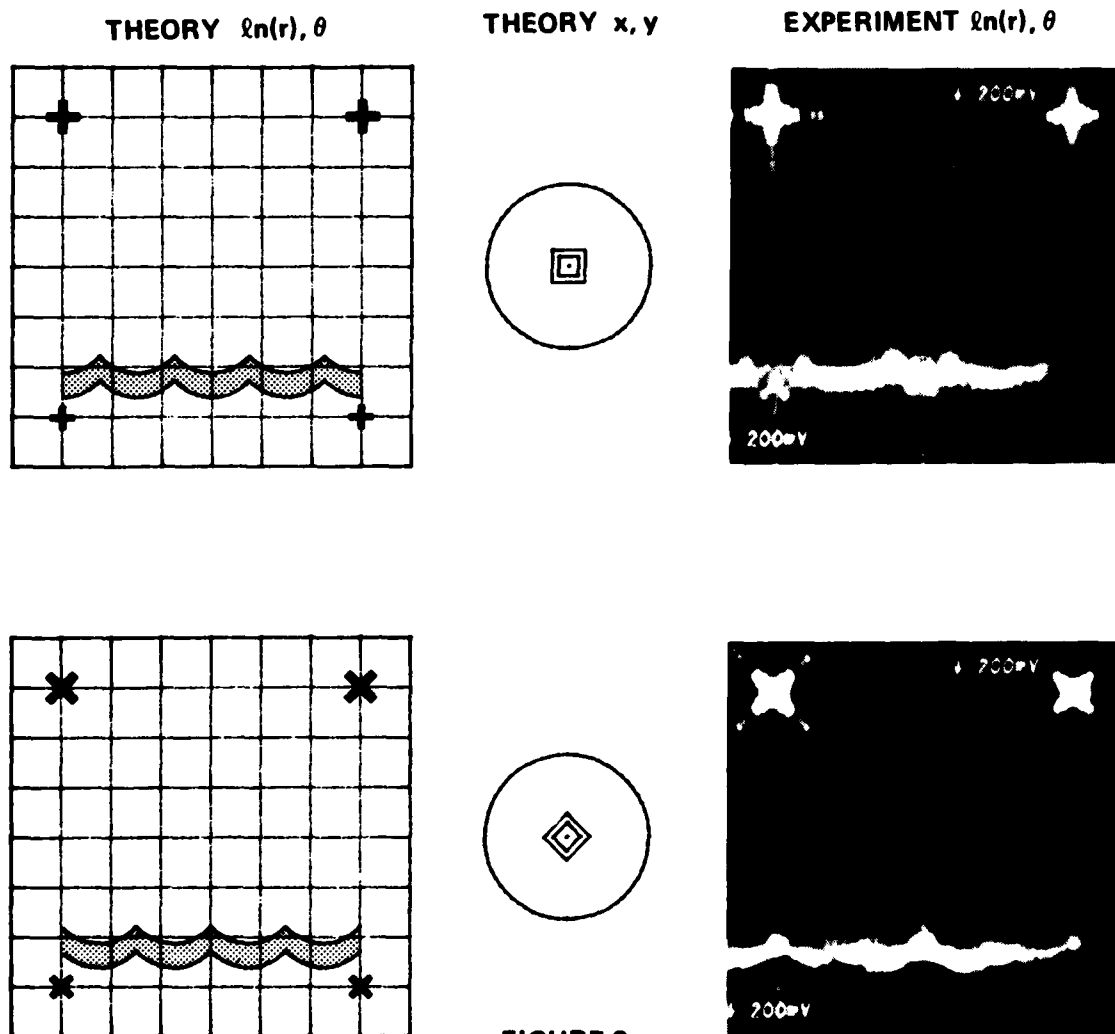


FIGURE 8

THE MELLIN TRANSFORM FILTER (MELLIN #1) ILLUMINATED BY A SQUARE ANNULUS ON AXIS AT VARIOUS ORIENTATIONS. COMPARISON OF EXPERIMENTAL DATA WITH THEORY. EACH SQUARE HAS DIMENSIONS OF $\pi/3$ IN EACH DIRECTION. $\ln(r)$ IS PLOTTED VERTICALLY, θ HORIZONTALLY. THE DOTS CORRESPOND TO THE DIFFRACTION PATTERN FROM THE CELL SIZE USED IN THE COMPUTER GENERATED HOLOGRAM

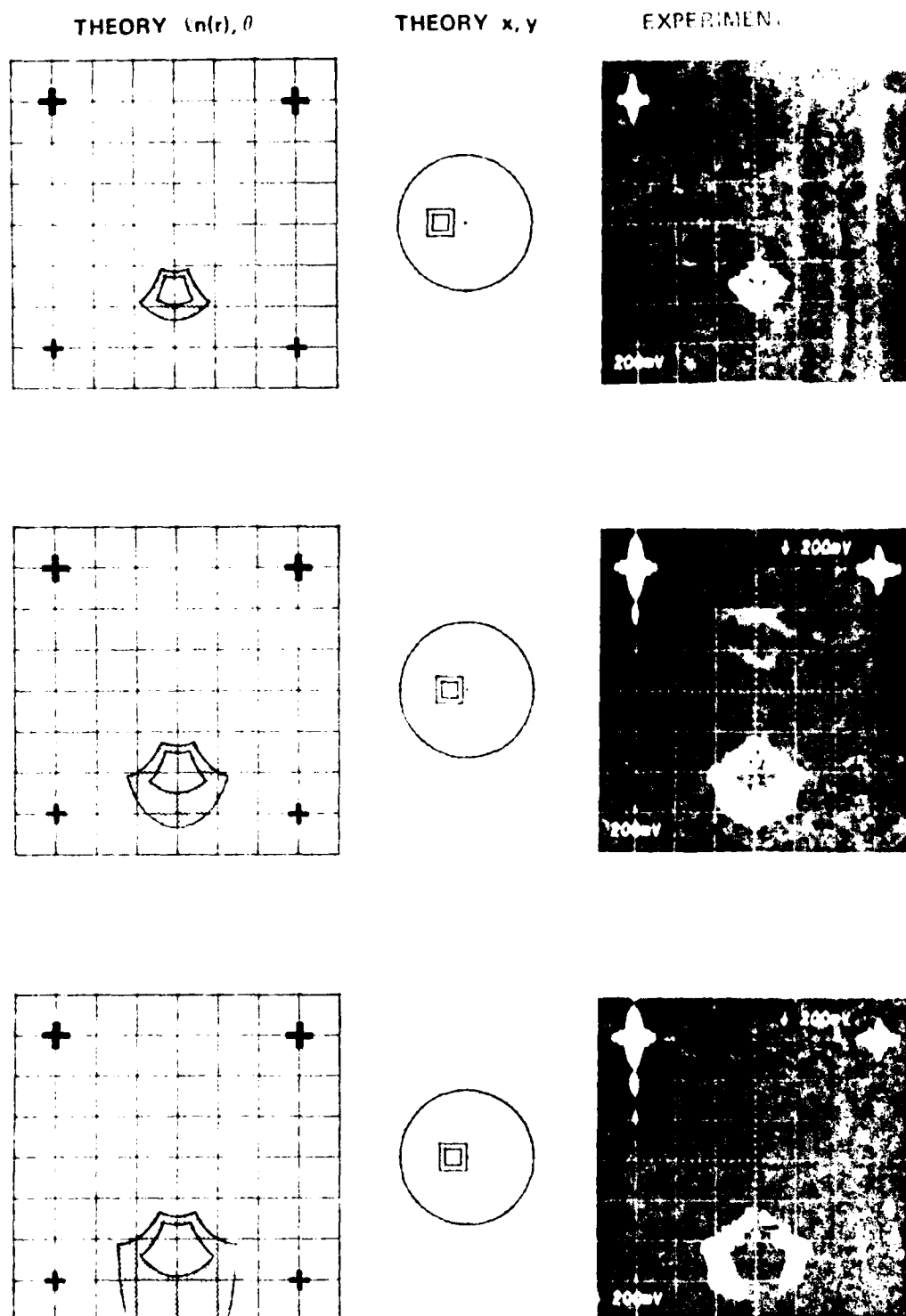


FIGURE 9

THE MELLIN TRANSFORM FILTER (MELLIN #1) ILLUMINATED BY A SQUARE ANNULUS OFF AXIS. COMPARISON OF EXPERIMENTAL DATA WITH THEORY. EACH SQUARE HAS DIMENSIONS OF $\pi/3$ IN EACH DIRECTION. $(n(r))$ IS PLOTTED VERTICALLY, θ HORIZONTALLY. THE DOTS CORRESPOND TO THE DIFFRACTION PATTERN FROM THE CELL SIZE USED IN THE COMPUTER GENERATED HOLOGRAM

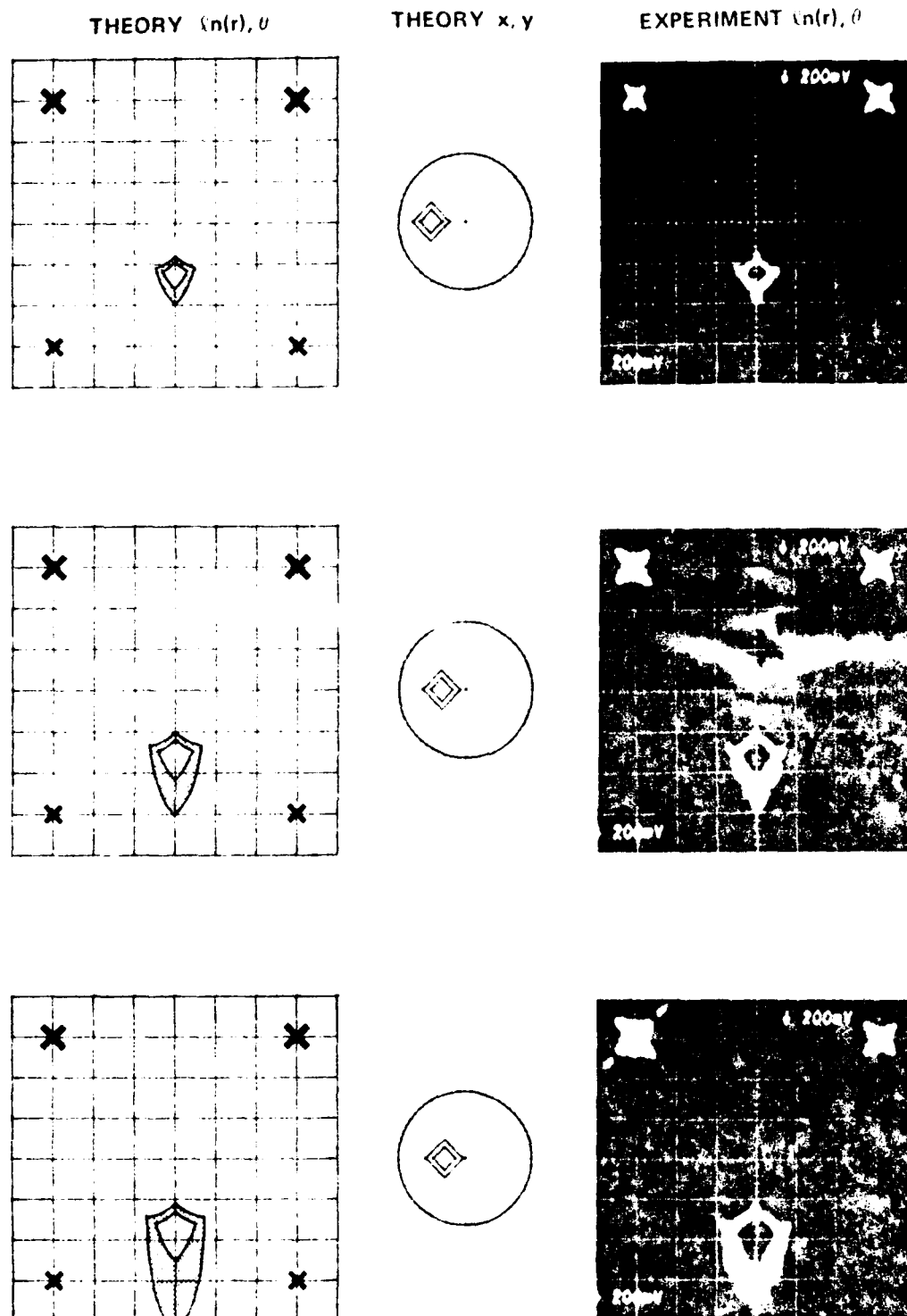
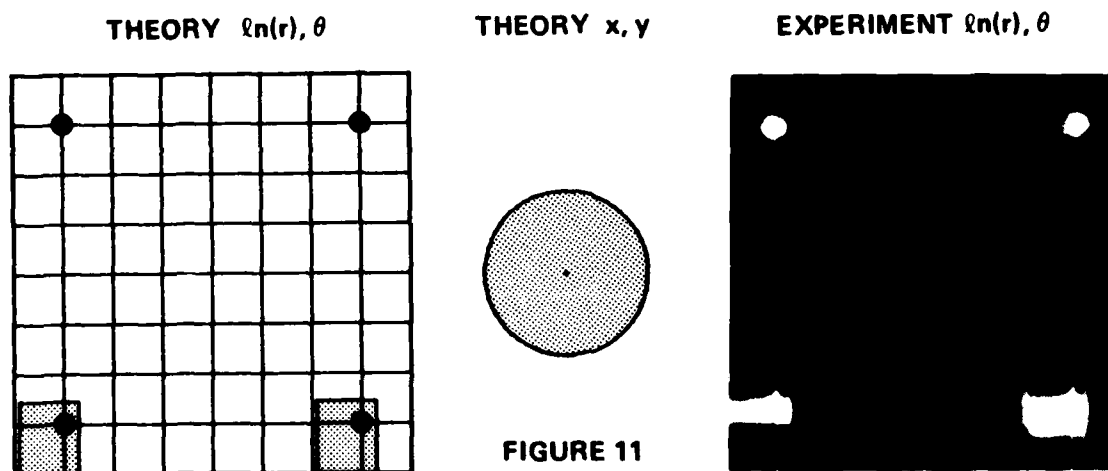


FIGURE 10

THE MELLIN TRANSFORM FILTER (MELLIN #1) ILLUMINATED BY A SQUARE ANNULUS OFF AXIS. COMPARISON OF EXPERIMENTAL DATA WITH THEORY. EACH SQUARE HAS DIMENSIONS OF $\pi/3$ IN EACH DIRECTION. $(n(r))$ IS PLOTTED VERTICALLY, θ HORIZONTALLY. THE DOTS CORRESPOND TO THE DIFFRACTION PATTERN FROM THE CELL SIZE USED IN THE COMPUTER GENERATED HOLOGRAM



THE MELLIN TRANSFORM FILTER (MELLIN #2) FULLY ILLUMINATED. COMPARISON OF EXPERIMENTAL DATA WITH THEORY. EACH SQUARE HAS DIMENSIONS OF $5\pi/3$ IN EACH DIRECTION. $\ell n(r)$ IS PLOTTED VERTICALLY, θ HORIZONTALLY. THE DOTS CORRESPOND TO THE DIFFRACTION PATTERN FROM THE CELL SIZE USED IN THE COMPUTER GENERATED HOLOGRAM

FIGS 4 to 11 (H/T)

APPENDIX A

SOME ALTERNATIVE GEOMETRIC TRANSFORMATIONS USING COMPUTER GENERATED HOLOGRAMS

In the text we have discussed the stationary phase method of realising a geometric transform where the phase function has a continuous form. In general this may not be always true and we must consider how a hologram may be constructed when this is not the case. One solution is to subdivide the hologram into subholograms^(2,10): where the phase variation within a subhologram is continuous but across subhologram boundaries need not be continuous. The format in which the subholograms appear depends critically on the style of transformation that is being attempted. For example Cederquist and Tai⁽²⁾ discuss the mapping of rings in the (x,y) plane to point along the v axis in the (u,v) plane.

$$\begin{pmatrix} x \\ y \end{pmatrix} \rightarrow \begin{pmatrix} u \\ v \end{pmatrix} = \begin{pmatrix} \sqrt{x^2+y^2} \\ 0 \end{pmatrix}$$

Clearly this transformation does not obey equation (4) in the main text and the phase is not continuous. The hologram was therefore divided into N concentric rings of average radius r_n and width Δr with

$$\phi(x,y) = 2\pi r_n x / \lambda f$$

for

$$|\sqrt{x^2+y^2} - r_n| \leq \Delta r/2$$

A similar transformation can be realised using the Mellin transform filter described in the text and a second hologram which transfers lines into points. Both of these hologram have continuous phase description and can potentially have a higher space-bandwidth product.

Other optical map transformations have been investigated by Bryngdahl⁽⁶⁾. The first case he considers is a preservation of geometric similarity

$$\begin{pmatrix} x \\ y \end{pmatrix} \rightarrow \begin{pmatrix} u \\ v \end{pmatrix} = \begin{pmatrix} x \\ y \end{pmatrix}$$

Use of equations (3) result in a phase function

$$\phi(x,y) = \frac{\pi}{\lambda f} (x^2+y^2)$$

which is, of course, the phase factor introduced by a lens of focal length f, ie a Fresnel zone-plate.

A second transformation described by Bryngdahl used the example

$$\begin{pmatrix} x \\ y \end{pmatrix} \rightarrow \begin{pmatrix} u \\ v \end{pmatrix} = \begin{pmatrix} p \exp(-x/q) \cos(y/q) \\ p \exp(-x/q) \sin(y/q) \end{pmatrix}$$

This transformation maps horizontal lines into circles of given radius, and vertical lines into radii. The phase function had the form

$$\phi(x,y) = - \frac{pq^2\pi}{\lambda f} \exp(-x/q) \cos(y/q)$$

The third transformation described by Bryngdahl involved using a chirped one dimensional grid structure for local modification of an image. Sections of an image could be extended to position relative to the features in the CGH.

APPENDIX B

PARAMETERS AND PROGRAMS USED TO DEFINE THE MELLIN TRANSFORM FILTERS DESCRIBED IN THE TEXT

$$\phi(x,y) = -\frac{2\pi s}{\lambda f} \left\{ y \tan^{-1}\left(\frac{y}{x}\right) - \frac{x}{2} \ln(x^2+y^2) + x + \pi y H(-x) \right\}$$

$$\begin{aligned} H(-x) &= 1 & x < 0 \\ H(-x) &= 0 & x > 0 \end{aligned}$$

$$\lambda = 514.5 \text{ nm}$$

$$f = 1000 \text{ mm}$$

$$\begin{aligned} s &= 5/2\pi & (\text{for Mellin Nos 1,3}) \\ s &= 1/2\pi & (\text{for Mellin No 2}) \end{aligned}$$

$$\Delta x = \Delta y = 102.9 \text{ } \mu\text{m}$$

$$c = 0.5 \text{ (see Figure 1)}$$

$$\begin{aligned} A_{nm} &= 1 & (r < 1 \text{ mm}) \\ A_{nm} &= 1/r & (r > 1 \text{ mm}) \end{aligned}$$

$$r(\text{max}) = 10.29 \text{ mm}$$

$$\begin{aligned} \text{Type of CGH} &- \text{type I} & (\text{for Mellin Nos 1,2}) \\ &\text{type II} & (\text{for Mellin No 3}) \end{aligned} \quad (\text{see Figure 1})$$

Bl: Mellin No 1

```

5 ! MELLIN # 1
10 PLOTTER IS 705
20 RAD
30 LIMIT 0,250,0,180
40 LOCATE 0,100*RATIO,0,100
50 SCALE -(12*RATIO),12*RATIO,-
  12,12
60 GOSUB 1000
70 PAUSE
1000 ! PLOT: DIM IN mm
1010 X1=.1029 @ ! X CELL SIZE
1020 Y1=.1029 @ ! Y CELL SIZE
1030 H1=.0026 @ ! MIN HEIGHT OF
  SLIT
1040 L=.0005145 @ ! WAVELENGTH 0
  F LIGHT
1050 F=1000 @ ! FOCAL LENGHT OF
  LENS
1060 C= 5 @ ! WIDTH OF SLIT
1070 R9=1 @ ! MIN RAD FOR AMP CO
  RR
◆1075 S=5/(2*PI) @ ! SCALE FACTOR
  FOR PHASE CALCULATION
1080 FOR X2=-100 TO 100
1090 X=X1*X2
1100 FOR Y2=-IP(SQR(10000-X2*X2)
  +1) TO IP(SQR(10000-X2*X2)+
  1)
1110 Y=Y1*Y2
1120 IF X2=0 AND Y2=0 THEN 1170
1130 GOSUB 2000
1140 IF A=0 THEN 1170
1150 GOSUB 3000
1160 GOSUB 4000
1170 NEXT Y2
1180 NEXT X2
1190 RETURN
2000 ! AMPLITUDE
2010 R=SQR(X^2+Y^2)
2020 IF R>R9*Y1/H1 THEN A=0 @ GO
  TO 2050
2030 IF R>R9 THEN A=R9/R @ GOTO
  2050
2040 A=1
2050 RETURN
3000 ! PHASE(REF SAITO)
3010 IF X2=0 THEN P=ABS(Y)*PI/2
  @ GOTO 3040
3020 P=Y*ATN(Y/X)-.5*X*LOG(X^2+Y
  ^2)+X
3030 IF X<0 THEN P=P+Y*PI
3040 P=-(2*PI*P*S/(L*F))
3050 P=ATN2(SIN(P),COS(P))
3060 RETURN
◆4000 ! HOLBAR
◆4010 Y5=A*Y1*.5
◆4020 C1=X+P*X1/(2*PI)
◆4030 Y8=Y+Y5
◆4040 Y9=Y-Y5
◆4060 X8=C1-X1/4
◆4070 X9=C1+X1/4
◆4110 GOSUB 5000
◆4120 RETURN
5000 MOVE X8,Y9
5010 DRAW X9,Y9
5020 DRAW X9,Y8
5030 DRAW X8,Y8
5040 DRAW X8,Y9
5050 PENUP
5051 FOR X7=X8 TO X9 STEP .01
5052 MOVE X7,Y9
5053 DRAW X7,Y8
5054 NEXT X7
5055 PENUP
5060 RETURN

```

B2: Mellin No 2

```

5 ! MELLIN # 2
10 PLOTTER IS 705
20 RAD
30 LIMIT 0,250,0,180
40 LOCATE 0,100,RATIO,0,100
50 SCALE -(12*RATIO),12*RATIO,-
    12,12
60 GOSUB 1000
70 PAUSE
1000 ! PLOT: DIM IN mm
1010 X1=.1029 @ ! X CELL SIZE
1020 Y1=.1029 @ ! Y CELL SIZE
1030 H1=.0026 @ ! MIN HEIGHT OF
    SLIT
1040 L=.0005145 @ ! WAVELENGTH O
    F LIGHT
1050 F=1000 @ ! FOCAL LENGHT OF
    LENS
1060 C=.5 @ ! WIDTH OF SLIT
1070 R9=1 @ ! MIN RAD FOR AMP CO
    EF
◆1075 S=1/(2*PI) @ ! SCALE FACTOR
    FOR PHASE CALCULATION
1080 FOR X2=-100 TO 100
1090 X=X1*X2
1100 FOR Y2=-IP(SQR(10000-X2*X2)
    +1) TO IP(SQR(10000-X2*X2)+
    1)
1110 Y=Y1*Y2
1120 IF X2=0 AND Y2=0 THEN 1170
1130 GOSUB 2000
1140 IF A=0 THEN 1170
1150 GOSUB 3000
1160 GOSUB 4000
1170 NEXT Y2
1180 NEXT X2
1190 RETURN
2000 ! AMPLITUDE
2010 P=SQR(X^2+Y^2)
2020 IF R>R9*Y1/H1 THEN A=0 @ GO
    TO 2050
2030 IF P>R9 THEN A=R9/R @ GOTO
    2050
2040 A=1
2050 RETURN
3000 ! PHASE(REF SAITO)
3010 IF X2=0 THEN P=ABS(Y)*PI/2
    @ GOTO 3040
3020 P=Y*ATN(Y/X)-.5*X*LOG(X^2+Y
    ^2)+X
3030 IF X<0 THEN P=P+Y*PI
3040 P=-(2*PI*P*S/(L*F))
3050 P=ATN2(SIN(P),COS(P))
3060 RETURN
◆4000 ! HOLBAR
◆4010 Y5=A*Y1*.5
◆4020 C1=X+P*X1/(2*PI)
◆4030 Y8=Y+Y5
◆4040 Y9=Y-Y5
◆4060 X8=C1-X1/4
◆4070 X9=C1+X1/4
◆4110 GOSUB 5000
◆4120 RETURN
5000 MOVE X8,Y9
5010 DRAW X9,Y9
5020 DRAW X9,Y8
5030 DRAW X8,Y8
5040 DRAW X8,Y9
5050 PENUP
5051 FOR X7=X8 TO X9 STEP .01
5052 MOVE X7,Y9
5053 DRAW X7,Y8
5054 NEXT X7
5055 PENUP
5060 RETURN

```

B3: Mellin No 3

```

5 ! MELLIN # 3
10 PLOTTER IS 705
20 RAD
30 LIMIT 0,250,0,180
40 LOCATE 0,100*RATIO,0,100
50 SCALE -(12*RATIO),12*RATIO,-
  12,12
60 GOSUB 1000
70 PAUSE
1000 ! PLOT: DIM IN mm
1010 X1=.1029 @ ! X CELL SIZE
1020 Y1=.1029 @ ! Y CELL SIZE
1030 H1=.0026 @ ! MIN HEIGHT OF
  SLIT
1040 L=.0005145 @ ! WAVELENGTH 0
  F LIGHT
1050 F=1000 @ ! FOCAL LENGHT OF
  LENS
1060 C=.5 @ ! WIDTH OF SLIT
1070 R9=1 @ ! MIN RAD FOR AMP CO
  RR
◆1075 S=5/(2*PI) @ ! SCALE FACTOR
  FOR PHASE CALCULATION
1080 FOR X2=-100 TO 100
1090 X=X1*X2
1100 FOR Y2=-IP(SQR(10000-X2*X2)
  +1) TO IP(SQR(10000-X2*X2)+
  1)
1110 Y=Y1*Y2
1120 IF X2=0 AND Y2=0 THEN 1170
1130 GOSUB 2000
1140 IF A=0 THEN 1170
1150 GOSUB 3000
1160 GOSUB 4000
1170 NEXT Y2
1180 NEXT X2
1190 RETURN
2000 ! AMPLITUDE
2010 R=SQR(X^2+Y^2)
2020 IF P>R9*Y1/H1 THEN A=0 @ GO
  TO 2050
2030 IF R>R9 THEN A=R9/R @ GOTO
  2050
2040 A=1
2050 RETURN
3000 ! PHASE(REF SAITO)
3010 IF X2=0 THEN P=ABS(Y)*PI/2
  @ GOTO 3040
3020 P=Y*ATN(Y/X)-.5*X*LOG(X^2+Y
  ^2)+X
3030 IF X<0 THEN P=P+Y*PI
3040 P=-(2*PI*P*S/(L*F))
3050 P=ATN2(SIN(P),COS(P))
3060 RETURN
◆4000 ! HOLBAR
◆4010 Y5=A*Y1*.5
◆4020 C1=X+P*X1/(2*PI)
◆4030 Y9=Y+Y5
◆4040 Y9=Y-Y5
◆4050 IF P<-(PI/2) THEN GOTO 4080
◆4060 IF P>PI/2 THEN GOTO 4100
◆4070 X9=C1-X1/4 @ X9=C1+X1/4 @ G
  OSUB 5000 @ RETURN
◆4080 X8=X-X1/2 @ X9=C1+X1/4 @ GO
  SUB 5000
◆4090 X8=C1+3*X1/4 @ X9=X+X1/2 @
  GOSUB 5000 @ RETURN
◆4100 X8=C1-X1/4 @ X9=X+X1/2 @ GO
  SUB 5000
◆4110 X9=X-X1/2 @ X9=C1-3*X1/4 @
  GOSUB 5000 @ RETURN
◆4120 RETURN
5000 IF X9-X8<H1 THEN 5060
5005 MOVE X8,Y9
5010 DRAW X9,Y9
5020 DRAW X9,Y8
5030 DRAW X8,Y8
5040 DRAW X8,Y9
5050 PENUP
5051 FOR X7=X8 TO X9 STEP .01
5052 MOVE X7,Y9
5053 DRAW X7,Y8
5054 NEXT X7
5055 PENUP
5060 RETURN

```

DOCUMENT CONTROL SHEET

Overall security classification of sheet ... UNCLASSIFIED

(As far as possible this sheet should contain only unclassified information. If it is necessary to enter classified information, the box concerned must be marked to indicate the classification eg (R) (C) or (S))

1. DRIC Reference (if known)	2. Originator's Reference Memorandum 3874	3. Agency Reference	4. Report Security Classification Unclassified	
5. Originator's Code (if known)	6. Originator (Corporate Author) Name and Location Royal Signals and Radar Establishment			
5a. Sponsoring Agency's Code (if known)	6a. Sponsoring Agency (Contract Authority) Name and Location			
7. Title THE MELLIN TRANSFORM FILTER: A COMPUTER GENERATED HOLOGRAM				
7a. Title in Foreign Language (in the case of translations)				
7b. Presented at (for conference papers) Title, place and date of conference				
8. Author 1 Surname, initials West C L	9(a) Author 2	9(b) Authors 3,4...	10. Date 08 1985	pp. ref.
11. Contract Number	12. Period	13. Project	14. Other Reference	
15. Distribution statement UNLIMITED				
Descriptors (or keywords)				
continue on separate piece of paper				
Abstract The procedure for designing a detour phase computer generated holograms is described with particular reference to a scale and rotation invariant transformation filter known as a Mellin transform filter. Experimental results are presented which demonstrate the main features of the devices.				

END
FILMED

5-86

DTIC